



**HAL**  
open science

# Granular phase change materials for thermal energy storage: experiments and numerical simulations

Mohamed Rady

► **To cite this version:**

Mohamed Rady. Granular phase change materials for thermal energy storage: experiments and numerical simulations. Applied Thermal Engineering, 2010, 29 (14-15), pp.3149. 10.1016/j.applthermaleng.2009.04.018 . hal-00614642

**HAL Id: hal-00614642**

**<https://hal.science/hal-00614642>**

Submitted on 14 Aug 2011

**HAL** is a multi-disciplinary open access archive for the deposit and dissemination of scientific research documents, whether they are published or not. The documents may come from teaching and research institutions in France or abroad, or from public or private research centers.

L'archive ouverte pluridisciplinaire **HAL**, est destinée au dépôt et à la diffusion de documents scientifiques de niveau recherche, publiés ou non, émanant des établissements d'enseignement et de recherche français ou étrangers, des laboratoires publics ou privés.

## Accepted Manuscript

Granular phase change materials for thermal energy storage: experiments and numerical simulations

Mohamed Rady

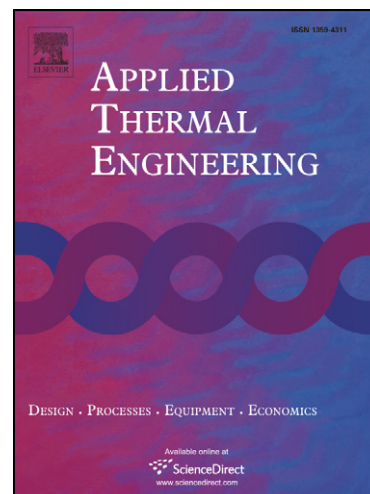
PII: S1359-4311(09)00126-4  
DOI: [10.1016/j.applthermaleng.2009.04.018](https://doi.org/10.1016/j.applthermaleng.2009.04.018)  
Reference: ATE 2785

To appear in: *Applied Thermal Engineering*

Received Date: 17 December 2008  
Revised Date: 4 March 2009  
Accepted Date: 7 April 2009

Please cite this article as: M. Rady, Granular phase change materials for thermal energy storage: experiments and numerical simulations, *Applied Thermal Engineering* (2009), doi: [10.1016/j.applthermaleng.2009.04.018](https://doi.org/10.1016/j.applthermaleng.2009.04.018)

This is a PDF file of an unedited manuscript that has been accepted for publication. As a service to our customers we are providing this early version of the manuscript. The manuscript will undergo copyediting, typesetting, and review of the resulting proof before it is published in its final form. Please note that during the production process errors may be discovered which could affect the content, and all legal disclaimers that apply to the journal pertain.



**GRANULAR PHASE CHANGE MATERIALS FOR THERMAL ENERGY STORAGE:  
EXPERIMENTS AND NUMERICAL SIMULATIONS**

Mohamed Rady\*

Mechanical Engineering Department, High Institute of Technology, Benha University,  
Benha 13 512, Benha, Egypt  
(Email: makrady@yahoo.com)

**Abstract**

The present article reports on the utilization of granular phase change composites (GPCC) of small particle diameter (1-3 mm) in latent heat thermal energy storage (LHTES) systems. The phase changing parameters (phase change temperature, latent heat, and energy storage capacity) of GPCC have been determined using differential scanning calorimeter (DSC) and temperature-history methods. Further analysis of measurement results has been conducted to describe the evolution of latent heat with temperature during phase change in terms of liquid fraction-temperature relationships. Charging and discharging packed bed column experiments have been also carried out for different operating conditions to analyze the potential of GPCC for packed bed thermal energy storage. The present column results clearly demonstrate the dependence of temperature variation along the packed bed and the overall performance of the storage unit on the phase change characteristics of GPCC. Small and non-uniform particles diameters of GPCC and heterogeneity of the bed material complicate the phenomena of heat transfer and evolution of latent heat in the packed bed. Mathematical modeling of the packed bed that considers the GPCC and air as two separate phases with inter-phase heat transfer is presented. Comparisons between experimental and numerical results are used to evaluate the sensitivity of numerical simulations to different model parameters.

---

\* Currently visiting professor: TREFLE, ENSCPB, University of Bordeaux, F33607 Pessac Cedex, France, rady@enscpb.fr

## Nomenclature

$c_p$	specific heat at constant pressure [J/(kg K)]	$T$	temperature (K)
$d$	Particle diameter (m)	$T_m$	phase change temperature (K)
$D$	packed bed column diameter (m)	$U_d$	Darcy velocity (m/s)
$f$	friction factor	$Z$	distance along the bed height (m)
$f_l$	liquid fraction	<b>Greek symbols</b>	
$G_\gamma$	mass flux [kg/(m <sup>2</sup> s)]	$\varepsilon$	porosity; volume fraction
$h_{sa}$	fluid-to-particle heat transfer coefficient [W/(m <sup>2</sup> K)]	$\mu$	air dynamic viscosity (kg/m s)
$H$	enthalpy (J/kg)	$\nu$	air kinematic viscosity (m <sup>2</sup> /s)
$H_{ls}$	PCM latent heat of fusion (J/kg)	$\rho$	density (kg/m <sup>3</sup> )
$k$	thermal conductivity [W/(m K)]	<b>Subscripts</b>	
$L$	bed height (m)	$a$	air
$Nu$	Nusselt number	$d$	dispersion
$P$	pressure (Pa)	$i$	inlet conditions
$Pe$	Peclet number	$0$	initial
$Pr$	Prandtl number of gas	$s$	solid
$Re$	Reynolds number		
$S$	volume specific surface area (m <sup>2</sup> /m <sup>3</sup> )		
$t$	time (s)		

## 1. Introduction

Research on advanced materials and systems for latent heat thermal energy storage (LHTES) has been intensified in recent years as due to the increasing interest in the design and development of energy-efficient building and the greater use of natural and renewable energy sources for heating, ventilation and cooling applications [1]. Different types of storage units have been conceived and studied. They differ by the nature of phase change material (PCM) and geometry of the unit. Storage of thermal latent heat in packed bed of spheres, containing each a PCM, provides direct heat exchange between the PCM and the heat transfer fluid. The analysis of packed beds thermal energy storage has been the subject of intensive research work [2, 3]. A recent review on the heat transfer characteristics of thermal energy storage systems using PCM capsules [4] shows that most of the previous studies have been limited to packed beds of spheres or cylinders containing PCM with large characteristic diameter in the order of few centimetres. In recent years, granular phase changing composites (GPCC) obtained by micro or macro-encapsulating PCMs in highly porous solid structures with protecting envelopes have been developed using different encapsulation techniques [5]. A wide range of GPCC in the form of particles of small diameters in the order of few millimetres are available that are suitable for low temperature energy storage applications.

Utilization of granular phase change composites (GPCC) of small particle diameter (1-3 mm) in latent heat thermal energy storage (LHTES) systems is the main concern of the present study. The motivations of the present interest in these materials are related to expected advantages in terms of heat transfer rates, flexibility, and multiplicity of applications in energy systems offered by using such GPCCs of small particle diameter (see Section 7 for a general overview). Potentials of their application have been recently investigated in desiccant cooling systems [6] and in air conditioning systems of buildings [7].

RUBITHERM GR27 and GR41 GPCC materials have been chosen for the present investigation [8]. They are considered as two examples representative of GPCC materials and the

results obtained in the present study are useful in evaluating the application of such materials in LHTES systems and highlighting difficulties associated with characterization and modeling. The composition of the granule is 65% ceramics and 35% paraffin wax by weight with 1-3 mm particle diameter. GPCC materials offer the advantage of maintaining their macroscopic solid form during phase change. The PCM is bound within a secondary supporting structure (polymer or ceramic) that ensures that the PCM, when in the liquid form, does not leak out of the granulate. The result is that the bound PCM is always a "dry" solid product and liquid handling is eliminated.

In the process development stage of a LHTES system, the knowledge of thermophysical properties of materials used for latent heat storage is essential for design and optimization. The quantity of thermal energy possible to store depends on the enthalpy variation in the working temperature range. Also, the enthalpy function or the apparent heat capacity of the PCM has to be known in order to obtain sufficiently accurate results in numerical simulations. This should take into account the temperature range over which the phase transition occurs under real operating conditions.

Difficulties in the characterization of GPCC are related to the specific nature of the material and heterogeneity of the sample and require special care and improvements in the analysis of measurement results. Moreover, small and non-uniform particles diameters of GPCC and heterogeneity of the bed material complicate the phenomena of fluid-particle heat transfer and evolution of latent heat in the storage packed bed. Studies on the utilization of GPCC taking into account these phenomena are important for successful integration in LHTES systems. The present study aims at providing experimental data on the characterization of phase changing parameters of GPCC and highlights the difficulties and required improvements in the measurement methods. Packed bed column experiments during charging and discharging modes have been carried out for different operating conditions to analyze the potential of GPCC for packed bed thermal energy storage and provide experimental data for comparison with numerical simulation. Comparisons between experimental and numerical results have been also carried out to show the sensitivity of their agreement to parameters concerning phase

change characteristics of GPCC, bed porosity, heat transfer correlations between the particle and fluid, and axial dispersion.

## 2. Materials Characterization

Differential scanning calorimetry (DSC) and a modified T-history method have been used to study the phase changing behavior of granular composites. Details on the experimental set-up and data analysis for GR27 and GR41 can be found in [9]. Characterizing granulate PCMs using DSC requires special care to assure that the thermophysical properties of samples (1–10 mg) are those of the bulk materials. The main difficulty of DSC characterization of granular PCM lies in the heterogeneity and structure of the sample as it significantly affects the details of the heat transfer between the sample pan and PCM material. Direct utilization of the measured DSC curves could result in an inexact representation of the sample enthalpy change. A simple procedure has been advised to obtain accurate results from the DSC measurements based on the estimation of the thermal resistance between the sample and its enclosure [9]. The thermal resistance between the GPCC sample and its container is evaluated using DSC measurements obtained at three different values of cooling/heating rates. Estimation of the thermal resistance allows correcting the measured DSC heat flux and calculation of corresponding correct sample temperature. The corrections are found to be significant at high values of heating/cooling rates and within the phase change temperature range of GPCC. High DSC heating or cooling rates promote the development of thermal and chemical non-equilibrium effects inside the sample material and result in an increase in the temperature range for melting and solidification. The latent heat of phase change is found to be essentially independent on the DSC heating/cooling rate.

The T-history method is an alternative simple and low cost technique for characterization of PCMs. In the original T-history method [10], the PCM sample and a sample with known thermal properties (distilled water) of the same initial homogeneous temperature are suddenly subject to ambient air with a room temperature which can be time dependent. Their temperature history upon cooling down is recorded.

Comparison of both curves, using a mathematical description of the heat transfer, allows the determination of the heat capacity of the solid and liquid phases and the latent heat of fusion of the PCM sample from the known specific heat of the reference material.

Using the T-history method, further modifications and improvements are employed to handle granular materials undergoing phase change over a temperature range. The accuracy of the original T-history method is shown to be limited by the assumption of constant temperature independent specific heats and the difficulty of determining the limits of solid and liquid phases. The concept of enthalpy and its relationship with temperature has been employed in the analysis to overcome these difficulties. Enthalpy-temperature and apparent heat capacity curves similar to those obtained using DSC have been developed for the GPCC, see Figs. 1 and 2. Characterization results for GR27 and GR41 are shown in Table 1. These include the start and end temperatures of phase change ( $T_{m1}$ ,  $T_{m2}$ ), the specific heat of solid and liquid phases ( $c_{ps}$ ,  $c_{pl}$ ), and the latent heat of phase change ( $H_{ls}$ ) which is the difference in enthalpy at temperature  $T_{m2}$  and  $T_{m1}$ . The values of  $T_{m1}$  and  $T_{m2}$  are obtained from the apparent heat capacity curve in a manner similar to the analysis of the heat flux-temperature curve using DSC.

GR27 and GR41 have approximately equal values of latent heat of phase change. The phase change temperature range of the two materials is interesting for low temperature LHTES applications. It should be noted that, the evolution of latent heat with temperature during phase change differs for the two materials. As compared to GR41, GR27 is characterized by the evolution of a considerable amount of latent heat over a narrower temperature range (22-27 °C). The evolution of latent heat for GR41 is more distributed over the phase change temperature range (31-45 °C).

### 3. Packed-bed Experiments

A schematic diagram of the experimental set-up used in this study is illustrated in Figure 3. The packed column is made of cylindrical PVC tube of 45 mm inside diameter and 2.5 mm wall thickness. The instrumented test section is 200 mm height. The bed test section is insulated with glass wool of 5 cm thickness. The packing (storage medium) is GR 27 or GR41 granulates of (1-3 mm) particle diameter. Airflow is produced by a centrifugal blower with variable mass flow rate. After passing through the PCM packed bed, it is exhausted from the top and then the flow rate is measured using a variable area float meter. The inlet air is heated by electrical heaters and mixed so that the temperature profile at the inlet bed is uniform. Copper constantan thermocouples of 0.1 mm diameter are used to measure the temperature at specific locations inside the test section, as shown in Figure 3. Air temperatures are also measured at the inlet and at the outlet of the test section. The bed temperature is uniform at the beginning of each experiment. For charging process, the experiment starts by switching on the electric heaters with the required power and allows for hot air flow at the desired rate to enter into the column. For discharging, the electric heater is switched off to allow for cold air flow into the column. Data acquisition system connected to the personal computer allows a continuous record of the temperature variation with time at the specified time interval.

Figures 4 and 5 show the time variation of temperature of the inlet air and at 4 cm from the bed inlet (locations T1 and T8 in Figure 3). The Reynolds number ( $Re$ ) is calculated based on the Darcy velocity at the inlet of the test section ( $U_d$ ) and using an average particle diameter of  $d=2$  mm,  $Re_d = U_d d / \nu$ . During charging of GR27 column, see Fig. 4, the bed temperature increases relatively rapidly in the initial stage of the process below the melting temperature range. In the range between 22 °C and 27 °C, the rate of increase in bed temperature decreases as due to the phase change of GR27. After the end of melting process, the rate of increase in bed temperature is high.

During discharging (solidification of GPCC), the variation of bed temperature flattens around 27 °C as due to phase change. Figure 5 shows the results for GR41 column which exhibits a lower flattening of the temperature profile during phase change. These results are compatible with GR27 and GR41 enthalpy-temperature variations obtained during material characterization using DSC and T-history methods. The observed phase change temperatures from the experiments agree with the results from the characterization experiments. It is also interesting to note that the measured temperatures T1 and T8 show negligible differences during the sensible heat change period. The differences between T1 and T8 are remarkable at the onset of phase change during melting and at the end during solidification. Small radial temperature difference during sensible heating and cooling periods are attributed as due to the heterogeneous nature of the bed particles that are manifested as local variations in the bed porosity. Minor changes in the PCM content of GPCC may be responsible for the remarkable temperature differences at the beginning and end of phase change.

#### 4. Mathematical Modeling

Detailed modeling of the heat transfer and fluid flow processes that take place in such arrangement of GPCC is quite complex. The rate of heat transfer to or from the solid in the packed bed is a function of the physical properties of the fluid and the solid, the flow rate of the fluid, and the physical characteristics of the packed bed. The overall heat transfer consists of the following modes: (1) the convective heat transfer from the walls of the packed bed tank to the fluid; (2) the convective heat transfer from the particles to the fluid flowing through the bed; (3) the conduction heat transfer from the walls of the bed to the particles constituting the bed; (4) the conduction heat transfer between the individual particles in the bed; (5) radiant heat transfer and (6) heat transfer by mixing of the fluid. In beds with adiabatic wall conditions, the radial conduction as well as the bed to wall surface heat transfer may be assumed to be small and negligible. Adiabatic wall conditions,

often used in industrial practice, are assumed in this study as due to the employed thermal insulation of the wall.

The governing equations for heat transfer in the packed bed are obtained by considering a representative elementary volume (REV) containing GPCC particles and air with volume fractions  $\varepsilon_s$  and  $\varepsilon_a$ , ( $\varepsilon_s + \varepsilon_a = 1$ ). They consist of the fluid and solid (GPCC) energy equations and take into account the thermodynamic non-equilibrium between the two phases of different temperatures ( $T_a$ ,  $T_s$ ). The air flow passing through the porous bed is considered to be steady and uniform with superficial (Darcy) velocity,  $U_d$ . Heat conduction in the wall material, of small thickness and thermal conductivity, and radiant heat transfer, for the present low differences in temperature, are assumed to be negligible. The air and GPCC energy equations are written as [11]:

$$\frac{\partial(\rho_a \varepsilon_a c_{pa} T_a)}{\partial t} + \frac{\partial \rho_a U_d c_{pa} T_a}{\partial z} = \frac{\partial}{\partial z} \varepsilon_a k_a \frac{\partial T_a}{\partial z} + h_{sa} S_{sa} (T_s - T_a) \quad (1)$$

$$\frac{\partial(\rho_s \varepsilon_s c_{ps} T_s)}{\partial t} = \frac{\partial}{\partial z} \varepsilon_s k_s \frac{\partial T_s}{\partial z} - h_{sa} S_{sa} (T_s - T_a) - \rho_s H_{fs} \varepsilon_s \frac{\partial f_l}{\partial t} \quad (2)$$

The inter-phase heat transfer is described by the heat transfer coefficient ( $h_{sa}$ ). The evolution of latent heat during phase change of the GPCC is accounted for by using the source term  $\rho_s H_{fs} \varepsilon_s \partial f_l / \partial t$  in Eq. (2). Where  $f_l$  is the liquid fraction of GPCC undergoing phase change and  $H_{fs}$  is the latent heat of fusion of the PCM material. The value of  $f_l$  is related to the temperature  $T_s$  and determines the rate of evolution of latent heat during phase change.

Knowledge of fluid-to-particle heat transfer coefficient  $h_{sa}$  is an important issue for the analysis of heat transfer in packed beds. A considerable amount of research work has been carried out in the literature to identify suitable correlations for the particle to fluid heat transfer coefficient. Numerous correlations for predicting heat transfer coefficients in packed beds exist in the literature [12-17]. A simple analysis of heat conduction from an isolated spherical particle surrounded by a

stagnant fluid leads to the conclusion that the limiting value of Nusselt number for low Reynolds number flows is 2.0. At higher Reynolds convective effects become significant and a correlation of the form  $Nu=f(Pr, Re)$  is to be expected. Correlations based on the Ranz model [18] and Galloway and Sage [19] have been widely used for heat transfer modelling in packed beds [3, 11]. The Ranz model provides a method of applying convection correlations for single spheres in an external flow to spheres in packed beds. With the Ranz model, the superficial velocity  $U_d$  is multiplied by a factor of 10.73 to yield an effective free stream velocity inside the packing. Thus the Reynolds number velocity of  $10.73U_d$  is used with convection correlations for single spheres to predict convection coefficients in packed beds. Ranz determined the factor 10.73 analytically and verified it by comparison with experimental results. The Nusselt number correlation using Ranz model [18] is written as:

$$Nu = (1.2 + 0.53 Re^{0.54}) Pr^{0.3} \quad (3)$$

Galloway and Sage [19] developed the following correlation for fluid-to-particle heat transfer coefficient in packed beds.

$$Nu = 2.0 + c_1 Re_d^{1/2} Pr^{1/3} + c_2 Re_d Pr^{1/2} \quad (4)$$

Where  $Re_d = U_d d / \nu$  and  $Pr = \nu / \alpha$ . For randomly packed bed of spheres  $c_1$  and  $c_2$  are 1.354 and 0.0326, respectively. Beasley and Clark [11] used higher values of these coefficients ( $c_1=2.031$  and  $c_2=0.049$ ), resulting in an increase of about 50% in the heat transfer coefficient, and obtained better agreement between the numerical and experimental results.

In the application of the above expressions for heat transfer, it is important to note that the axial dispersion coefficients as due to axial mixing must be properly estimated. There are two main mechanisms which contribute to axial dispersion: molecular diffusion and turbulent mixing arising from the splitting and recombination of flows around the particles. The effective thermal conductivity of the fluid phase consists of the stagnant and the dispersion conductivity.

$$k_{a\text{eff}} = k_a + k_d \quad (5)$$

The dispersive component of the longitudinal thermal conductivity in the porous media was evaluated as function of the Peclet number [20, 21] as follows:

$$k_d = 0.022k_a \frac{Pe_d^2}{1-\epsilon} \quad (Pe_d < 10)$$

$$k_d = 2.7k_a \frac{Pe_d}{\epsilon^{1/2}} \quad (Pe_d > 10) \quad (6)$$

To complete the mathematical description of the present problem, the initial and boundary conditions are specified as follows: at  $t=0$ :  $T_a=T_s=T_o$ , at  $z=0$ :  $T_a=T_{in}$ ,  $\partial T_s / \partial z = 0$ , at  $z=L$ :  $\partial T_s / \partial z = \partial T_a / \partial z = 0$ . Where  $T_o$  is the initial bed temperature and  $T_{in}$  is the inlet air temperature.

## 5. Numerical Solution

Examination of the governing equations (1) and (2) shows that the liquid fraction  $f_l$  represents an extra unknown that is known only after the solution for solid temperature  $T_s$ . Therefore, an iterative technique has been adopted for the calculation of  $f_l$  as follows,

$$f_l^{i+1} = f_l^i + \xi \quad \text{where the correction} \quad \xi = \frac{c_{ps}(T_s - T_m)}{H_f} \quad (7)$$

Where  $i$  is the iteration number and the constraints  $f_l^{i+1} = \max[0.0, f_l^{i+1}]$  and  $f_l^{i+1} = \min[1.0, f_l^{i+1}]$  are forced. At convergence  $\xi=0$  and the temperature of phase changing nodes is equal to the phase change temperature  $T_m$ . It should be mentioned that the correction term  $\xi$  takes the form of Stefan number. Previous simulations of packed beds reported in the literature have been concerned with phase changing materials at constant temperature  $T_m$ . In such cases, the value of  $f_l$  changes from zero to one during melting at  $T_s=T_m$ . However, the present characterization of GPCC shows that the phase change process takes place over a temperature range (between  $T_{m1}$  and  $T_{m2}$ ).

The value of  $T_m$  used in Eq.(7) is therefore function of the liquid fraction  $T_m=f(f_l)$ . This functional relationship is a characteristic of the phase change material as explained afterwards.

Equations (1) and (2) are discretized by using the finite volume method employing an implicit time scheme. The upwind scheme is used for discretization of the convection terms and the central difference scheme is used for discretization of the diffusion terms. The resulting equations are solved using the Gauss–Seidel iteration method. A time step of 0.001 s and a grid mesh of 0.1 mm are used in the simulations to ensure numerical stability and accuracy. The simulation results are independent of the grid size and time step used.

Figures 6 and 7 show complete comparisons of experimental (T1, T8, T3, T9, T7, Tout) and numerical simulation (T1 Sim, T3 Sim, T7 Sim, Tout Sim) results during charging of GR27 and GR41 columns. In these calculations, Ranz model for particle-to fluid heat transfer has been used, axial dispersion is calculated using Eqs. (5) and (6), an average bed porosity of 0.42 is used, and the phase changing characteristics resulting from the T-history method are employed for the functional relationship of liquid fraction and Temperature. The agreement between experimental and numerical results is reasonable. However, some differences are observed and need to be evaluated. These differences may be attributed due to uncertainty in the parameters of heat transfer model such as the phase change characteristics of GPCC, bed porosity, fluid-particle heat transfer coefficient, particle diameter, and axial dispersion. An analysis of the sensitivity of agreement between numerical and experimental results to these parameters is performed in next section in order to define the most critical model components.

## 6. Sensitivity of Agreement to Model Parameters

The sensitivity of numerical results to the values of particle-to-fluid heat transfer coefficient, dispersive component of thermal conductivity, and description of the phase change characteristics of GPCC are investigated. Numerical simulations have been carried out to evaluate the effects of these model components on the agreement between the experimental and numerical results. The effect of

each parameter is investigated separately and unless otherwise specified the parameters used in the above simulations of Figures 6 and 7 are used in the following simulations.

### **Effects of phase change characteristics:**

The evolution of latent heat during charging and discharging of LHTES unit as function of temperature is an important issue for modeling, optimization, and design of the unit. This evolution is expressed in terms of the variation of liquid fraction  $f_l$  of GPCC with temperature as follows.

$$f_l(T) = \frac{H(T) - H_s(T_{m1})}{H_{ls}} \quad (8)$$

$H(T)$  is the enthalpy at any temperature ( $T$ ) and  $H_s(T)$  is the solid phase enthalpy. Variations of  $f_l$  with temperature for GR27 and GR41 are obtained by further analysis of T-history and DSC measurements. Applications of different forms for the functional variation of liquid fraction with temperature in numerical simulations of packed beds may affect the bed performance characteristics.

Applications of different functions of  $f_l$ - $T$  results in different evolution of latent heat during phase change. Simulations have been also carried out using an assumed linear profile of  $f_l$ - $T$  between  $T_{m1}$  and  $T_{m2}$ , an assumption that is usually used to handle phase change over a temperature range, and comparisons have been made with the results obtained using measured  $f_l$ - $T$  curves obtained from the T-history and DSC. Figure 8 shows that the assumption of linear profiles of  $f_l$ - $T$  can induce remarkable differences in the predicted variation of bed temperature with time. The differences can be clearly distinguished during the phase change period. The results obtained using curves of T-history and DSC are close to the experimental measurements.

### **Effects of bed porosity:**

Packed bed porosity has been the subject of extensive research [22, 23]. Some of this research work has focused on developing correlations to predict overall void fraction for use in global prediction of pressure drop as function of the ratio of tube diameter to some effective particle

diameter,  $D/d$ . The average bed porosity is modeled by deKlerk [23] as an exponential decay function.

$$\varepsilon = \varepsilon_b + 0.35 \exp\left(-0.39 \frac{D}{d}\right) \quad (9)$$

The effect of the packing mode is embodied in the average bed porosity at infinite column diameter  $\varepsilon_b$ . Literature values vary for the bed voidage of a randomly packed bed of spheres at large column to particle diameter ratio. This variance is ascribed to the packing mode. Four random packing modes for spheres are distinguished: (a) very loose random packing ( $\varepsilon_b \approx 0.44$ ) obtained by gradual defluidization of a fluidized bed or by sedimentation; (b) loose random packing ( $\varepsilon_b \approx 0.40$ -0.41) obtained by letting spheres roll individually in place, or by dropping the spheres into the container as a loose mass; (c) poured random packing ( $\varepsilon_b \approx 0.375$ -0.391) obtained by pouring spheres into a container; and (d) dense random packing ( $\varepsilon_b \approx 0.359$ -0.375) obtained by vibrating or shaking down the packed bed. Due to the stochastic nature of the packing process, accurate and reliable predictions of bed porosity are elusive. The sensitivity of numerical predictions to the value of bed porosity is shown in Fig. 9. Comparisons of experimental and numerical results obtained using different values of bed porosity show that the effect of bed porosity is significant. The local changes in porosity can lead to large variations in predicted velocity profile and therefore non-uniform head loss along the packed bed. The accurate prediction of local porosity is therefore important for predicting heat transfer in packed beds. This is especially true for packed beds having a particle size and shape distribution as the present application. It seems that some form of multidimensional statistical description of the packing will be necessary for performance modeling. The average bed to particle diameter employed in the present study  $\approx 25$  provides a central region essentially free from the wall effect on void fraction. However, near the walls, the void fraction increases and may result in flow channeling.

**Effects of fluid-to-particle heat transfer coefficient and axial dispersion:**

Uncertainty of the fluid-particle heat transfer coefficient is related to the correlations existing in the literature. For example, the widely used correlations given by Eqs.(3) and (4) for Ranz model and Galloway and Sage [19] result in heat transfer coefficient that differ by about 15%. Also, the importance of axial dispersion should be evaluated. Another source of uncertainty can be attributed as due to the assumption of uniform particle diameter. Screen analysis of GR27 and GR41 shows that they contain 0,1% of particles with diameter  $d_p > 4$  mm, 7,5% with  $d_p = 3,0 - 4,0$  mm, 89,5% with  $d_p = 1,0 - 3,0$  mm, 2,3% with  $d_p = 0,5 - 1,0$  mm, and 0,6% with  $d_p < 0,5$  mm. Therefore, a mean particle diameter of 2 mm has been assumed for the purpose of numerical simulations. The particle non-uniform shape may affect the boundary layer and probably increase the heat transfer coefficient.

Simulations have been carried out to evaluate the effects of uncertainty of these model parameters on the agreement between numerical and experimental results. It has been found that the utilization of Ranz model and Galloway and Sage [19] correlation for estimation of the fluid-to-particle heat transfer coefficient has no remarkable effect on the agreement between numerical and experimental results. Also, simulations results using different particle diameter of 1.5 mm are very similar to those obtained using a particle diameter of 2 mm as an average value. This can be explained by the fact that decreasing particle diameter decreases the heat transfer coefficient as due to the decrease of Reynolds number. On the other hand, the surface area for heat exchange between the particles and fluid increases with the decrease of the particle diameter. The final effect, within the uncertainty limits of particle diameter, is a small variation of the heat exchange rates between the particles and fluid that is manifested in unremarkable differences in the agreement between the experimental and numerical results. The effects of axial dispersion have been also evaluated by comparison of results obtained with and without axial dispersion. The results indicate that, for the

range of Reynolds number studied, the longitudinal thermal dispersion has no significant contribution to the overall temporal thermal response of the packed bed.

## 7. General overview for LHTES applications

An analysis of the role of the characteristic diameter of PCM capsule in a packed bed thermal energy storage system is an essential issue that explains the importance, limitations, and advantages of utilization of GPCC of small characteristic diameter. The goal of an energy storage system is to obtain high heat transfer rates during charging and discharging with reasonable pumping requirements. Applying heat exchangers principles [24] and introducing the column diameter ( $D$ ) as a characteristic length, the number of transfer units (NTU) can be written as:

$$NTU = \frac{hA}{\dot{m} c p_a} = \frac{6h(1-\varepsilon)D}{d \rho_a U_d c p_a} = 6 St(1-\varepsilon) \frac{D}{d} \quad (10)$$

Where  $\dot{m}$  is the mass flow rate of air,  $A$  is the total surface area of heat transfer,  $h$  is the particle to fluid heat transfer coefficient, and  $St$  is the Stanton number ( $St = Nu/Re.Pr$ ). The functional dependence of heat transfer coefficient on Reynolds number based on particle diameter ( $Re$ ) is given by Eq. (4). NTU is a dimensionless parameter whose magnitude influences the unit performance. High values of NTU result in enhancing the unit effectiveness with high charging and discharging rates. The pressure gradient along the bed length can be obtained from a modified form of the Ergun equation [25, 26].

$$-\frac{\partial p}{\partial z} = \frac{150\mu(1-\varepsilon)^2}{d^2 \varepsilon^3} U_d + 1.75 \frac{\rho(1-\varepsilon)}{d \varepsilon^3} U_d^2 \quad (11)$$

Equations (11) can be written in dimensionless form by introducing the definition of friction factor ( $f$ ) and considering the pressure drop per unit length of column ( $\Delta P/L$ ) as:

$$f = \frac{\Delta P(D/L)}{\rho U_d^2} = \left(\frac{D}{d}\right) \frac{(1-\varepsilon)}{\varepsilon^3} \left[ \frac{150(1-\varepsilon)}{Re} + 1.75 \right] \quad (12)$$

Equations (10) and (12) are used to investigate the variation of NTU and pressure drop along the bed considering air as the heat transfer fluid at different values of PCM capsule diameter. In order to

make this analysis, one has to consider a constant Reynolds number based on the column diameter ( $Re_o = \rho U_d D / \nu$ ), assume different values of  $D/d$ , calculate ( $Re = Re_o d/D$ ), and then employ Eq. (10) to estimate NTU and Eq. (12) to calculate  $\Delta P(D/L)$ .

Figure 10 shows the variation of NTU and pressure drop along the bed with  $D/d$  for different values of Reynolds number ( $Re_o$ ). It can be observed that the value of NTU increases with the decrease of Reynolds number ( $Re_o$ ). For the same value of  $Re_o$ , the value of NTU increases with the decrease of particle diameter (increase of  $D/d$  ratio) as due to the increase of heat transfer surface area. The rate of increase of NTU with the increase of  $D/d$  is higher at low values of Reynolds number. Concerning the pressure drop, high values of pressure drop are obtained with the increase of  $Re_o$ . The rate of increase of pressure drop with the increase of  $D/d$  ratio is lower at low values of Reynolds number. This analysis shows that, in general, utilization of encapsulated PCM of small particle diameter is advantageous in terms of heat transfer rates and pumping requirements at low values of Reynolds number ( $Re_o$ ). Limitations of high pressure drop at high values of Reynolds number can be overcome by employing systems of small characteristic length (compact systems). Using GPCCs of small particle diameter may be useful when limited volumes of energy storage are applicable. The storage granulate offers the clear advantage that it can be used to fill containers of any conceivable geometry (flexibility in applications). The granulate form of the latent heat storage material provides the large surface area required for effective heat transfer.

## CONCLUSION

Utilization of granular phase change composites (GPCC) of small particle diameter (1-3 mm) in latent heat thermal energy storage (LHTES) systems is the main concern of the present study. Experimental measurements using DSC and T-history methods are carried out for characterization of phase changing parameters of GPCC such as phase change temperature, latent heat, and energy storage capacity. The evolution of latent heat with temperature during phase change in terms of

liquid fraction-temperature relationships is described. Difficulties and required improvements in the measurement methods to handle GPCC are discussed. Packed bed column experiments during charging and discharging modes are carried out for different operating conditions to analyze the potential of GPCC for packed bed thermal energy storage and provide experimental data for comparison with numerical simulation.

The present column results clearly demonstrate the dependence of temperature variation along the packed bed and the overall performance of the storage unit on the phase change characteristics of GPCC. Small and non-uniform particles diameters of GPCC and heterogeneity of the bed material complicate the phenomena of heat transfer and evolution of latent heat in the packed bed. Mathematical modeling of the packed bed that considers the GPCC and air as two separate phases with inter-phase heat transfer is presented. Comparisons between experimental and numerical results show an important sensitivity of their agreement to the phase change characteristics of GPCC and estimation of bed porosity. The sensitivity of agreement to the estimation of particle-to- fluid heat transfer coefficient and the axial dispersion are found to be less important. The functional variation of liquid fraction of GPCC with temperature during phase change is therefore an important parameter that controls the dynamics of packed bed during charging and discharging processes. Also, for packed beds having a particle size and shape distribution as the present application, accurate prediction of local porosity is essential for analysis of heat transfer in the bed. It seems that some form of multidimensional statistical description of the packing will be necessary for performance modeling. The present analysis is useful for practical applications in the design and optimization of LHTEs system using GPCC during the process development stage and for performance evaluation of packed bed latent heat storage columns. In general, utilization of encapsulated PCM of small particle diameter is advantageous in terms of heat transfer rates and pumping requirements for applications involving low values of Reynolds number, compact systems, and systems with limited volume of energy storage.

**References**

- [1] Farid M., Khudhair A. M., Siddique A. K., Razack S. A. [2004], A review on phase change energy storage: materials and applications, *Energy Conversion and Management*, Vol. 45: pp. 1597-1615.
- [2] Ismail K., Henriquez J. [2002], Numerical and experimental study of spherical capsules packed bed latent heat storage system, *Applied Thermal Engineering*, Vol. 22: pp.1705-1716.
- [3] Benmansour A., Hamdan M. A., Bengueuddach A. [2006], Experimental and numerical investigation of solid particles thermal energy storage unit, *Applied Thermal Engineering*, Vol. 26: pp. 513-518.
- [4] Regin, F., Solanki, S.C., Saini, J. S., [2008], Heat transfer characteristics of thermal energy storage system using PCM capsules: A review, *Renewable and Sustainable Energy Reviews*, Vol. 12: pp. 2438-2458.
- [5] Zhang D., Zhou J., Wu K., Li Z. [2005], Granular phase changing composites for thermal energy storage, *Solar Energy*, Vol. 78: pp. 471-480.
- [6] Rady, M. A., Huzayyin, A. S., Arquis, E., Monneyron, P., Lebot, C. [2009], Study of heat and mass transfer in a dehumidifying desiccant bed with macro-encapsulated phase change materials, *Renewable Energy*, 34, pp. 718–726
- [7] Nagano K, Takeda S, Mochida T, Shimakura K, Nakamura T. [2006], Study of a floor supply air conditioning system using granular phase change material to augment building mass thermal storage-Heat response in small scale experiments. *Energy and Buildings*, Vol. 38, pp. 436-446.
- [8] RUBITHERM, <http://www.rubitherm.com/>
- [9] Rady, M. and Arquis, E. [2009], A comparative study of phase changing characteristics of granular phase changing materials using DSC and T-history methods, *Proceedings of the Fourth*

- International Conference on Thermal Engineering: Theory and Applications, January 12-14, 2009, Abu Dhabi, UAE.
- [10] Zhang J. Y. and Jiang Y. [1999], A simple method, the T-history method, of determining the heat of fusion, specific heat and thermal conductivity of phase-change materials. *Measurement & Science Technology*, Vol. 10, pp. 201-205.
- [11] BEASLEY, D. E. and CLARK, J. A. [1984], Transient response of a packed for thermal energy storage bed, *Int. J. Heat and Mass Transfer*, Vol. 27, pp. 1659-1669.
- [12] Baptista P. N., Oliveira, A. R., Oliveira, J. C., Sastry, S. K. [1997], Dimensionless analysis of fluid-to-particle heat transfer coefficients, *Journal of Food Engineering*, Vol. 31: pp. 199-218.
- [13] Sanderson T. M., Cunningham, G. T. [1995], Performance and efficient design of packed bed thermal storage systems. Part 1., *Applied Energy*, Vol. 50: pp. 119-132.
- [14] Galloway, T. R., Sage, B. H. [1970], A model of the mechanism of transport in packed distended and fluidised beds, *Chim. Eng. Sci.* 25 , p. 495.
- [15] Wakao, N., Kaguei, N., Funazkri, T. [1979], Effect of fluid dispersion coefficients on particle-to-fluid heat transfer coefficients in packed beds, *Chem. Eng. Sci.*, Vol. 34, pp. 325-336.
- [16] Nosfor, E. C., Adebisi, G. A. [2001], Measurements of the gas-particle convective heat transfer coefficient in a packed bed for high temperature energy storage, *Exp. Therm. And Fluid Sc.*, Vol. 24, pp. 1-9.
- [17] SESHADRI, Y. and PEREIRA, R. O. S. [1986], Comparison of formulae for determining heat transfer coefficient of packed beds, *Transactions ISIJ*, Vol. 26, pp. 604-610.
- [18] Ranz, W. E. [1952], Friction and transfer coefficients for single particles and packed beds. *Chem. Eng. Prog.*, Vol. 48:pp. 247-53.

- [19] Galloway, T. R., Sage, B. H. [1970], A model of the mechanism of transport in packed distended and fluidised beds, *Chim. Eng. Sci.* 25 , p. 495.
- [20] Kuwahara, F., Nakayama, A., Koyama, H. [1996], A numerical study of thermal dispersion in porous media. *Journal of Heat Transfer* Vol. 118, pp. 756–761.
- [21] Amiri, A., Vafai, K. [1998], Transient analysis of incompressible flow through a packed bed, *International Journal of Heat and Mass Transfer*, Vol. 41, pp. 4257-4279.
- [22] Theuerkauf, J., Witt, P., Schwesig, D. [2006], Analysis of particle porosity distribution in fixed beds using the discrete element method, *Powder Technology*, Vol. 165, pp. 92–99.
- [23] A. de Klerk [2003], Voidage variation in packed beds at small column to particle diameter ratio, *AIChE Journal*, Vol. 49, pp. 2022–2029.
- [24] Incropera, F. , DeWitt, D. [2006], *Fundamentals of Heat and Mass Transfer*, 5th Edition, John Wiley & Sons, Inc.
- [25] Ergun S. [1952], Fluid flow through packed columns, *Chem. Engng Prog.*, Vol. 48 (2), p. 89.
- [26] MacDonald, I. F. , El-Sayed, M. S. and Dullien, F. A. L. [1979], Flow through porous media- the Ergun equation revisited, *Ind. Engng Chem. Fundam.*, Vol. 18 (3), p. 199.

**List of Figures and Tables:**

Table 1. Characterization of GR27 and GR41 using the T-history method.

Fig. 1 Enthalpy and apparent specific heat variation with temperature for GR27.

Fig. 2 Enthalpy and apparent specific heat variation with temperature for GR41.

Fig. 3 Schematic of the experimental set-up for packed-bed.

Fig. 4 Variation of bed temperature during charging and discharging of GR27 column,  $Re = 7.29$ .

Fig. 5 Variation of bed temperature during charging and discharging of GR41 column,  $Re = 7.29$ .

Fig. 6 Comparison of experimental and numerical results, (GR27,  $Re = 7.29$ ).

Fig. 7 Comparison of experimental and numerical results, (GR41,  $Re = 7.29$ ).

Fig. 8 Comparison of experimental and numerical simulations using different liquid fraction functions, (GR27,  $Re = 7.29$ ).

Fig. 9 Comparison of experimental and numerical results, effects of bed porosity, (GR27,  $Re = 7.29$ ).

Fig. 10 Variation of NTU and pressure drop with PCM capsule diameter.

Table 1: Characterization of GR27 and GR41 using the T-history method.

Sample	$T_{m1}$ (°C)	$T_{m2}$ (°C)	$c_{ps}$ (J/kg.K)	$c_{pl}$ (J/kg.K)	$H_{ls}$ (J/kg)
GR27	21	29	2044	1921	64850
GR41	31	45	2784	2745	65895

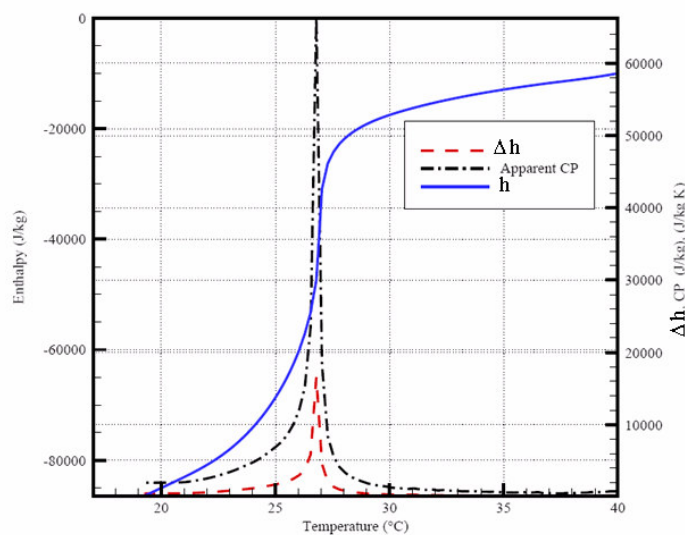


Figure 1: Enthalpy and apparent specific heat variation with temperature for GR27.

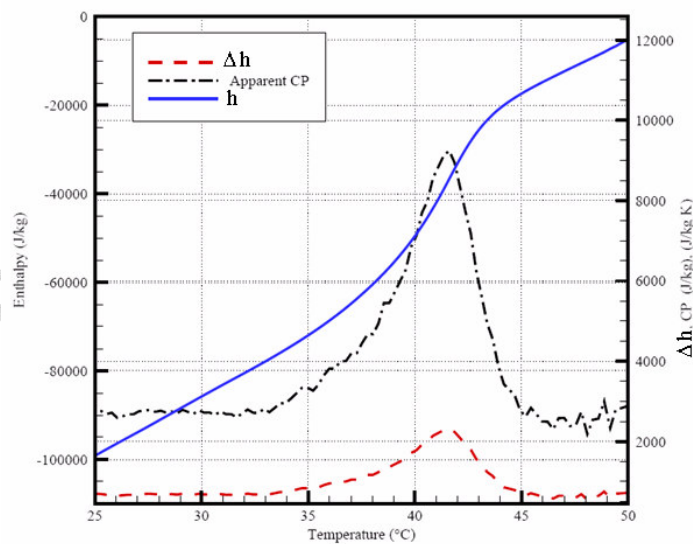


Figure 2: Enthalpy and apparent specific heat variation with temperature for GR41.

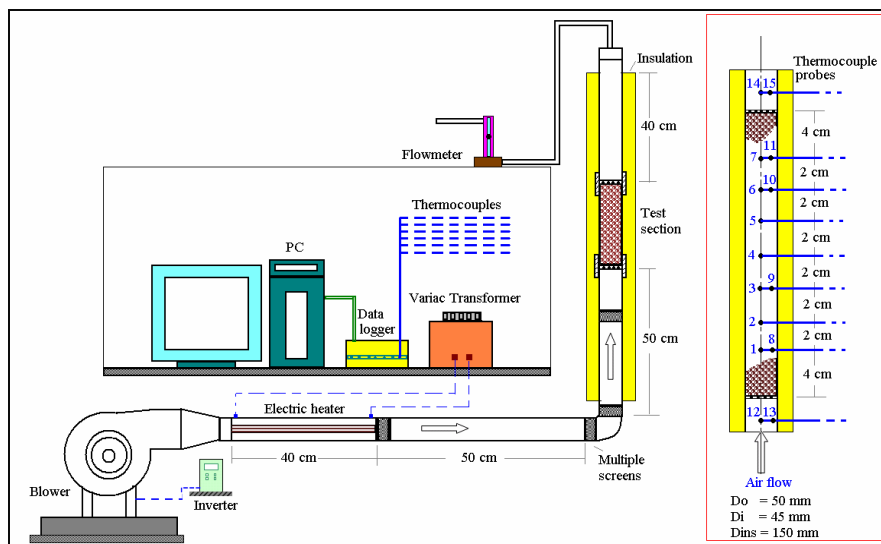


Figure 3: Schematic of the experimental set-up for packed-bed.

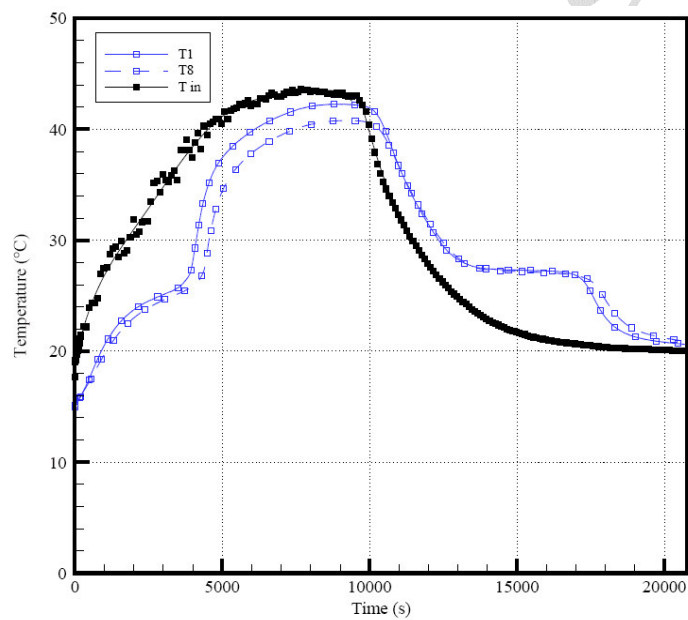


Figure 4: Variation of bed temperature during charging and discharging of GR27 column,  $Re = 7.29$ .

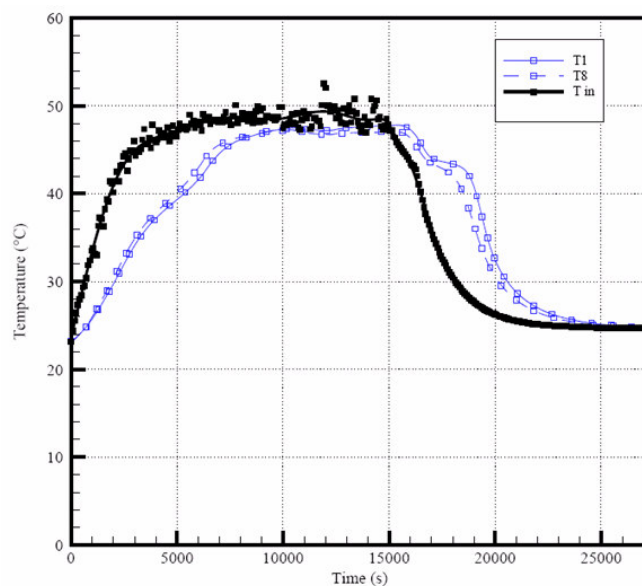


Figure 5: Variation of bed temperature during charging and discharging of GR41 column,  $Re = 7.29$ .

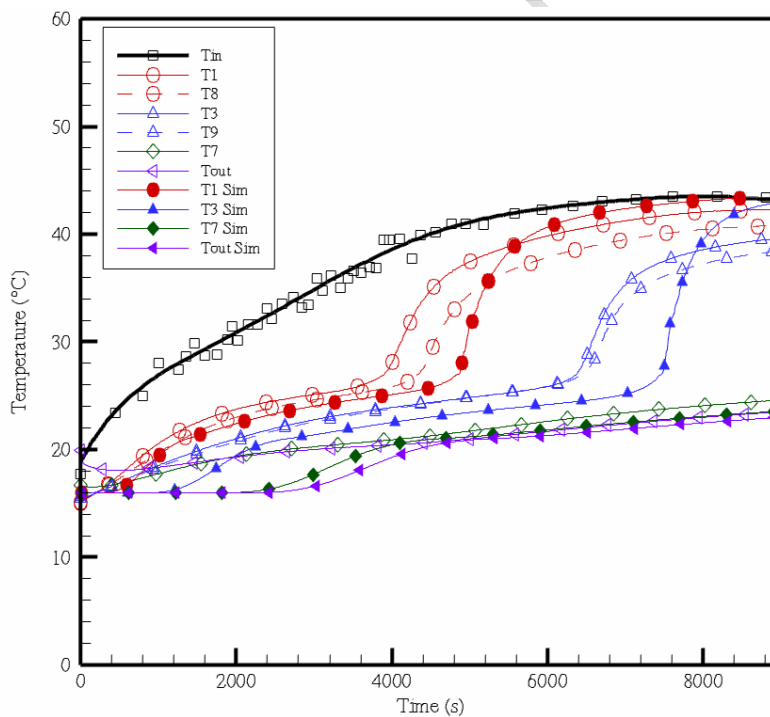


Figure 6: Comparison of experimental and numerical results, (GR27,  $Re = 7.29$ ).

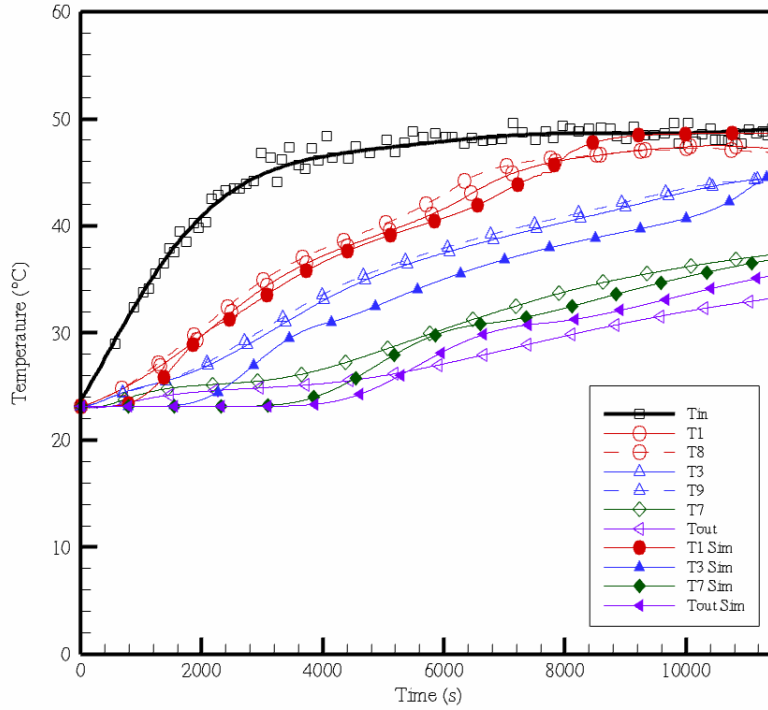


Figure 7: Comparison of experimental and numerical results, (GR41, Re=7.29).

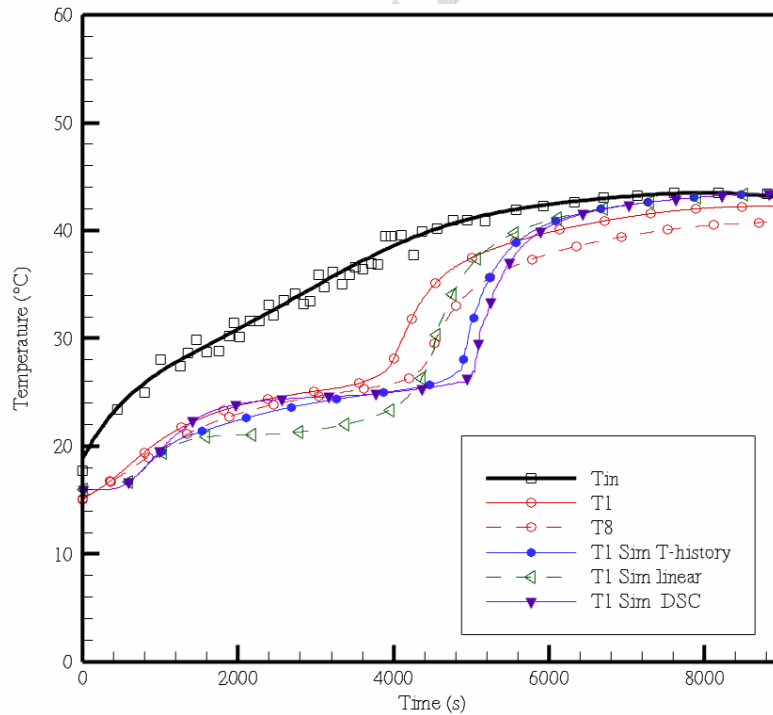


Figure 8: Comparison of experimental and numerical simulations using different liquid fraction functions, (GR27, Re=7.29).

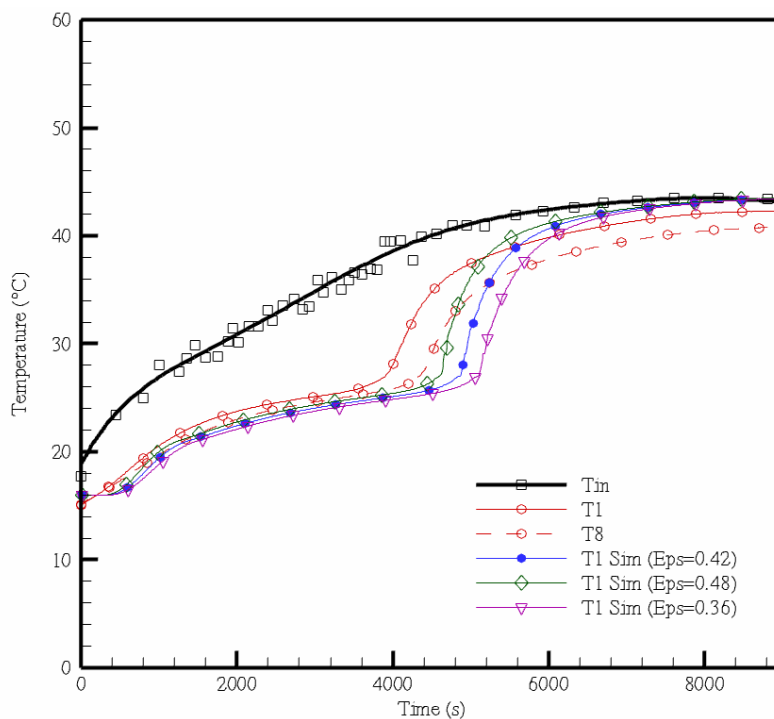


Figure. 9 Comparison of experimental and numerical results, effects of bed porosity, (GR27, Re=7.29).

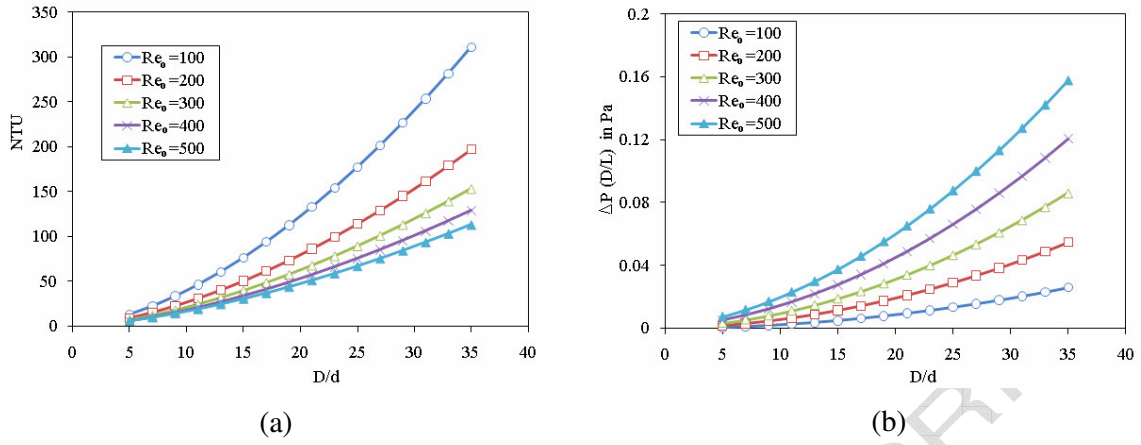


Figure 10: Variation of NTU and pressure drop with PCM capsule diameter